

## Effects of organic matter on uptake and intracellular trafficking of nanoparticles in *Tetrahymena thermophila*

Xiangrui Wang<sup>†</sup>, Dingyuan Liang<sup>†</sup>, Ying Wang<sup>†</sup>, Qingquan Ma<sup>†</sup>, Baoshan Xing<sup>‡</sup>,  
Wenhong Fan<sup>†, §, \*</sup>

### Preparation of SDS-alkyl-AgNPs with varied alkyl chain lengths

Citrate-capped AgNPs were first prepared according to Wan's work.<sup>1</sup> Then, the synthesized AgNPs (20 nm) were concentrated and purified via centrifugation at 50,000×g. The Ag concentration of citrate-capped AgNPs stock suspension was determined using ICP-MS and adjusted to 2 g/L with ultrapure water (Millipore, 18.2 MΩ). Then, hydrophobic AgNPs were prepared through ligand exchange, using a procedure based on Jana's work.<sup>2</sup> In a typical procedure, 6 mL of citrate-capped AgNPs was mixed with 24 mL ethanol, and a certain volume of mercaptan (hexanethiol, dodecanethiol, or octadecanethiol) was subsequently added with vigorous stirring. The molar ratio of thiol to silver was kept at 1:1. Then, 30 mL toluene was added and the stirring was continued for 10 min. Next, thiol coated AgNPs were precipitated by adding minimum ethanol. After washing, three different hydrophobic AgNPs with varied alkyl chain lengths were obtained through redispersion in trichloromethane.

In order to disperse the hydrophobic silver nanoparticles into aqueous system, a sodium dodecyl sulfate (SDS) bilayer structure was employed, as described in Li's work.<sup>3-5</sup> Briefly, a small

---

\*Corresponding author: School of Space and Environment, Beihang University NO.37 Xueyuan Road, Haidian District Beijing 100191, P.R. China Tel: (86)-10-61716810; Fax: (86)-10-82339571; E-mail: [fanwh@buaa.edu.cn](mailto:fanwh@buaa.edu.cn)

<sup>†</sup>School of Space and Environment, Beihang University, Beijing 100191, P.R. China

<sup>‡</sup>Stockbridge School of Agriculture, University of Massachusetts, Amherst, Massachusetts 01003, United States

<sup>§</sup>Beijing Advanced Innovation Center for Big Data-Based Precision Medicine, Beihang University, Beijing 100191, P.R. China

Electronic supplementary information (ESI) available

volume of SDS solution was added to the solution of hydrophobic AgNPs in trichloromethane to reach 5 mM concentration. Subsequently, 15 mL of hydrophobic AgNPs solution was mixed with 135 mL of ultrapure water, which resulted in an obvious phase separation. The mixture was then subjected to sonication via an ultrasonic probe for 5 min. After that, the turbid solution was centrifuged at  $600\times g$  for 5 min, at which point the AgNPs clearly transferred into the aqueous phase. The upper layer was then collected and centrifuged at  $100,000\times g$  for 30 min. Finally, the pellets with SDS bilayer were washed and dispersed with ultrapure water. The stock AgNPs suspension was eventually adjusted to 400 mg/L with ultrapure water and the Ag concentrations were determined using ICP-MS. Moreover, the coating mass and dissociative SDS mass ratio were determined using TOC analyzer (Multi N/C @2100, Analytik Jena AG), and the range of total SDS mass ratio was also estimated.

### Calculation of the coating mass, dissociative SDS mass ratio and total SDS mass ratio

The coating mass and dissociative SDS mass were both determined based on TOC concentration. Briefly, 250  $\mu\text{L}$  of SDS-alkyl-AgNPs was mixed with 750  $\mu\text{L}$  nitric acid for 1h. After that,  $C_T$  (mg/L) as the concentration of total organic carbon (TOC) in AgNPs stock solution was determined. Then another 250  $\mu\text{L}$  of SDS-alkyl-AgNPs was dropped into 750  $\mu\text{L}$  ultrapure water and centrifuged for 20 min at  $18000\times g$ . The TOC concentration of supernatant namely  $C_s$  (mg/L) was also detected. Therefore, the coating mass and dissociative SDS mass ratio could be expressed using the following formula:

$$f_{\text{coating}} = \frac{(C_T - C_s)}{100} \quad (1)$$

$$f_{\text{dissociative}} = \frac{C_s}{100} \quad (2)$$

Basically, the TOC concentration in AgNPs stock solution should be composed of alkyl group and SDS. Therefore, the total SDS mass ratio could be calculated using the follow formula:

$$f_{\text{total-SDS}} = \frac{C_T - C_{\text{alkyl}}}{100} \quad (3)$$

At the present study, the alkyl chain mass was hardly to detect, but the range of it could be estimated.

As for SDS-hexyl-AgNPs, the hexyl mass ratio should be less than  $f_{\text{coating}}^{\text{hexyl}}$ , which is 0.038. As for

SDS-dodecyl-AgNPs and SDS-octadecyl-AgNPs, the alkyl mass ratio should be less than  $2 \times f_{\text{coating}}^{\text{hexyl}}$ ,

$3 \times f_{\text{coating}}^{\text{hexyl}}$ , respectively. After all, the range of total SDS mass ratio could be estimated, as shown in

Table 1 in main text.

### Fitting curve using one-site binding model

The one-site binding model was developed based on chemical reaction equilibrium, which assumed that the complex had no residual fluorescence. Therefore, the association constant  $K_a$  could be expressed as:

$$K_a = \frac{(1 - \frac{F}{F_0}) \times C_0}{\frac{F}{F_0} \times C_0 \times [nC - (1 - \frac{F}{F_0}) \times C_0]} \quad (4)$$

where  $F$  and  $F_0$  are the fluorescence intensities of labelled BSA in the presence and absence of SDS-alkyl-AgNPs;  $C_0$  represents the concentration of labelled BSA and  $C$  represents the concentration of quencher;  $n$  represents the binding sites per quencher. The equation (4) could be simplified as the following equations:

$$C = \frac{C_0}{n} \times \frac{Q}{Q+1} + \frac{Q}{nK_a} \quad (5)$$

$$Q = \frac{F_0}{F} - 1 \quad (6)$$

The above equations established the relationship between  $C$  and  $Q$ . By a non-linear fitting, we could obtain the binding sites per NPs and the association constant  $K_a$ .

Usually, the Stern-Volmer equation (a linear fitting) was utilized to calculate the association constant in the fluorescence quenching experiment. However, this situation is only achieved if the added ligand concentration is at least 10 higher than the protein concentration.<sup>6</sup> The model we proposed here avoided such disadvantage, thus it would reflect the interaction between NPs and protein more really.

### Cytotoxicity test of silver nanoparticles

For the cell viability experiment,  $5 \times 10^4$  *T. thermophila* cells were added into a 96-well plate (Corning), followed by the addition of 10  $\mu$ L alamar blue solution. After incubation at 28 °C for 4 hours, the cells were diluted to 1 mL with ultrapure water. The characteristic fluorescence signal of reduced alamar blue ( $E_x/E_m=530/590$  nm) was measured. For the mitochondrial activity test,  $5 \times 10^5$  *T. thermophila* cells were collected through centrifugation ( $600 \times g$ , 5 min) to remove exposure media and suspended in 1 mL freshwater. Then, 80  $\mu$ L of *T. thermophila* solution was added into 120  $\mu$ L culture medium (containing 20  $\mu$ L CCK-8 solution) in a 96-well plate. After incubation at 28 °C for 3 hours, the OD450 was measured using a microplate reader. For ROS and MMP tests, the collected *T. thermophila* was incubated with fluorescent dye DCFH-DA (10  $\mu$ M) and JC-1, respectively. Healthy *T. thermophila* cells were also exposed to CCCP (10 mM) as the positive control group for MMP test. After 20 min of incubation at 28 °C, cells were gently washed with freshwater twice. Finally, *T. thermophila* cells were resuspended in 2 mL freshwater. The ROS fluorescence was measured at excitation/emission wavelengths of 480/523 nm using a Fluorescence Spectrophotometer F-7000 (Hitachi, Japan). MMP was measured based on the ratio of fluorescence intensities at emission wavelengths of 597 nm and 540 nm, with the excitation wavelength at 490 nm. For all the tests, three replicates were performed. Finally, all the results were expressed as a ratio to the control. Moreover, after being stained with JC-1, *T. thermophila* cells were fixed with formalin (final 0.4%) and DAPI dye solution. The nucleus and mitochondria were observed under a fluorescence microscope with violet and green light excitation, respectively. Finally, the photographs were merged to visualize the distribution of intact mitochondria.

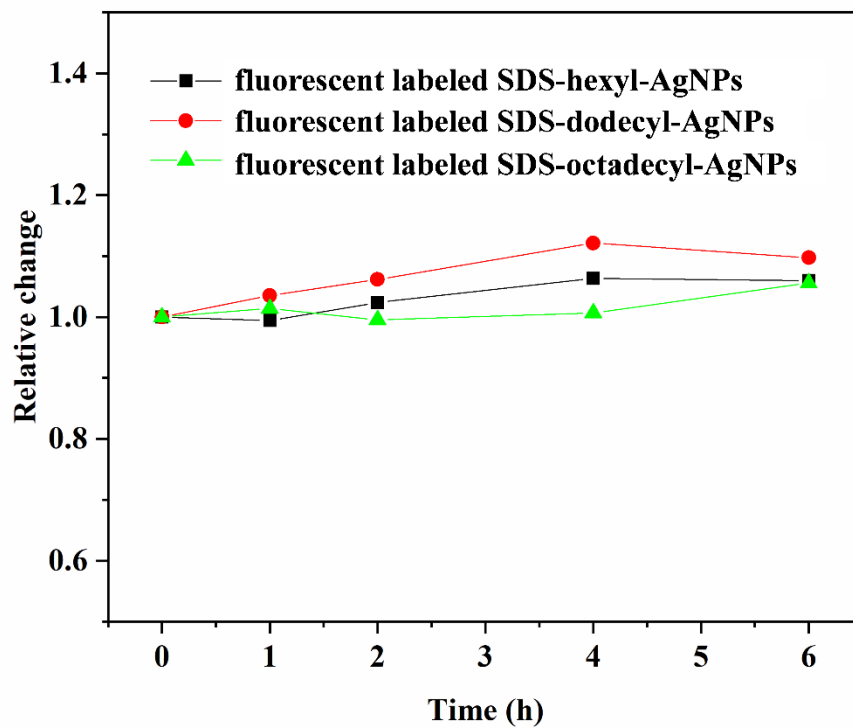


**Figure S1** The relative change of fluorescence ratio ( $E_m(\text{FITC})/E_m(\text{RBITC})$ ) of SDS-alkyl-AgNPs in the freshwater after 6 h exposure.

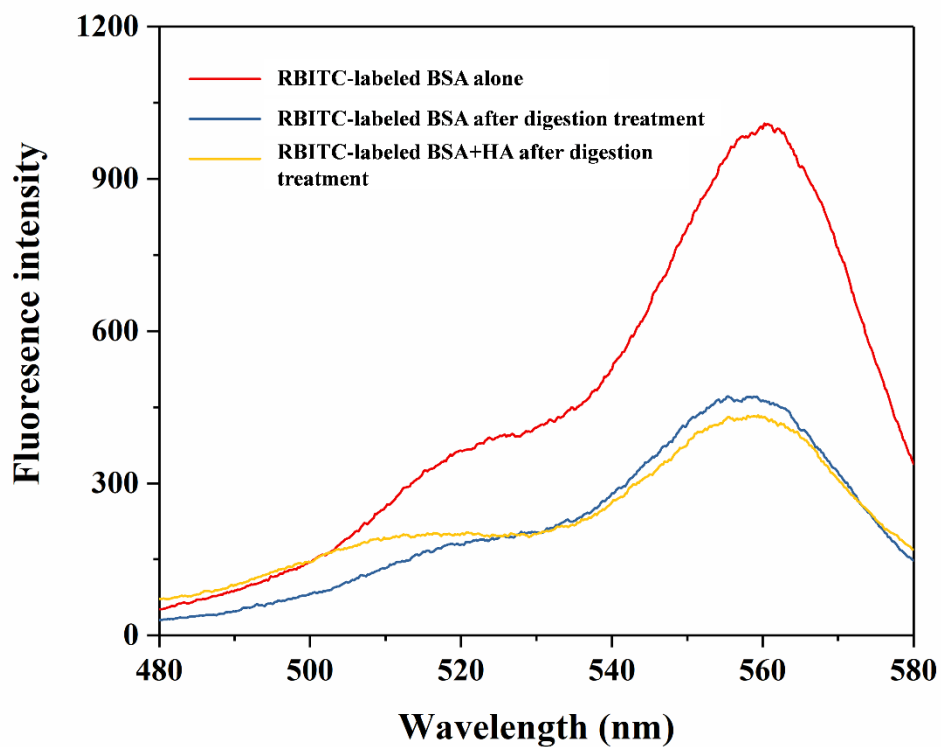


**Figure S2** The fluorescence intensity of 10 mg/L RBITC-labeled BSA alone, 10 mg/L RBITC-labeled BSA after digestion treatment and 10 mg/L RBITC-labeled BSA+ 20 mg/L HA after digestion treatment. The digestion treatment was conducted by adding organic matters into 2 mL of 2% v/v ammonium hydroxide solution and 0.15 mL of 30% H<sub>2</sub>O<sub>2</sub>. The mixed solution was then heated at 60°C for 30 min.

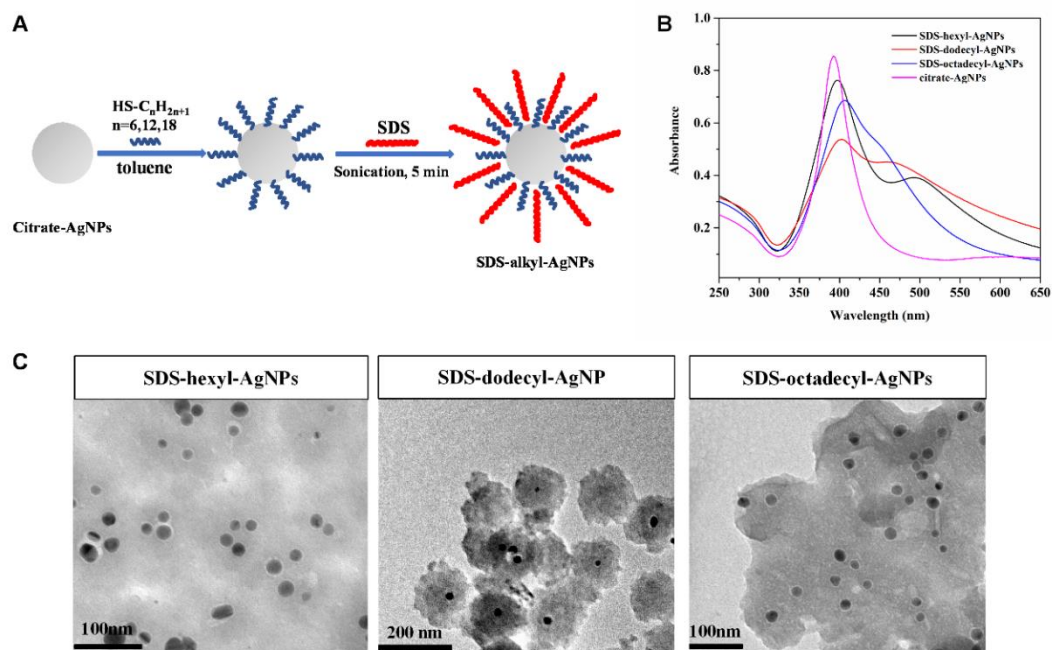


**Figure S3** A) Preparation of SDS-alkyl-AgNPs with various carbon chain lengths ( $n=6$ , hexyl;  $n=12$ , dodecyl;  $n=18$ , octadecyl). B) UV-vis spectra of SDS-alkyl-AgNPs and citrate-capped AgNPs in ultrapure water. C) Representative TEM images of SDS-alkyl-AgNPs.

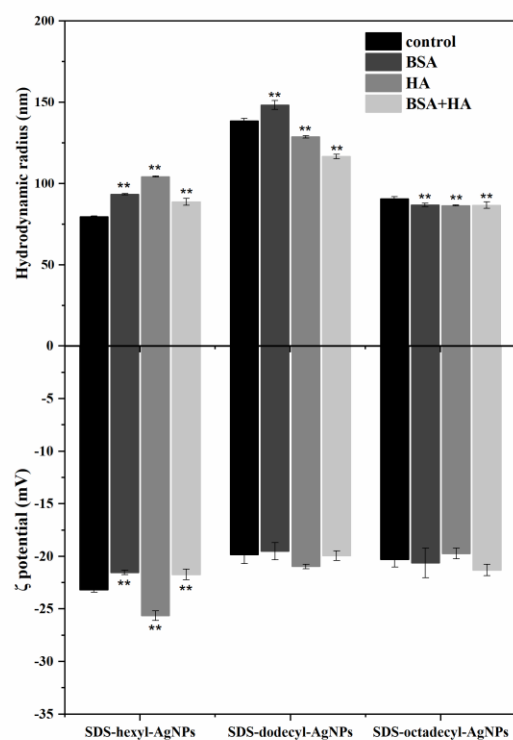


**Figure S4** The zeta potential and hydrodynamic radius of SDS-alkyl-AgNPs after mixing with BSA, HA or BSA and HA together. One-way ANOVA test was performed to compare statistically significant differences between nanoparticles in the presence of organic matter and nanoparticles alone. \*\* represents  $p < 0.01$ .

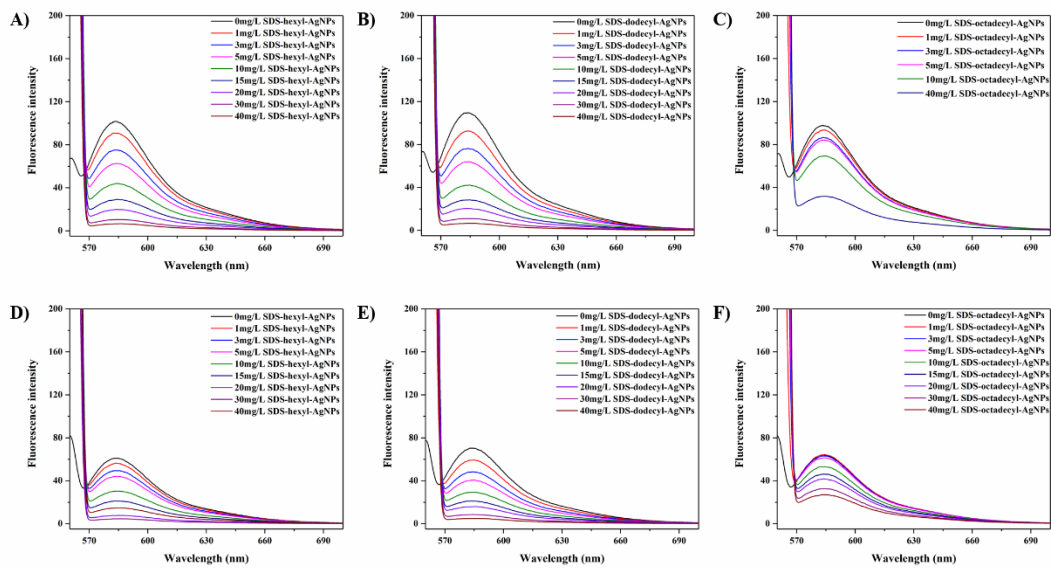


**Figure S5** The fluorescence quenching of BSA induced by SDS-alkyl-AgNPs alone (A-C) and in the presence of HA (D-F).

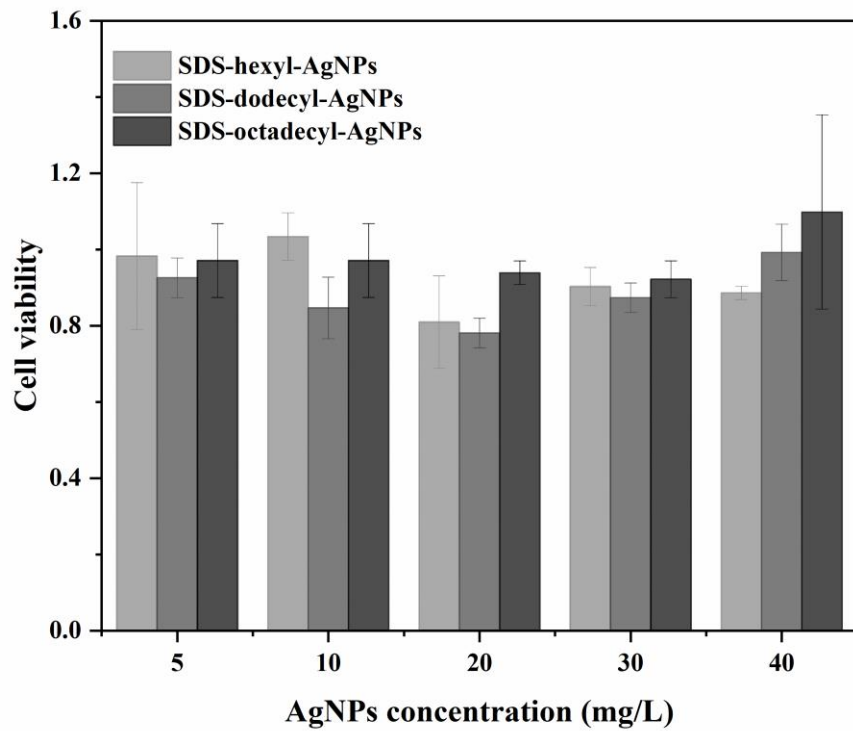


**Figure S6** The cell viability of *T. thermophila* cells using alamar blue assay after exposure with different concentration of SDS-alkyl-AgNPs. One-way ANOVA test was performed to compare statistically significant differences at different exposure concentration, which found that there was no mortality in all the exposure groups.

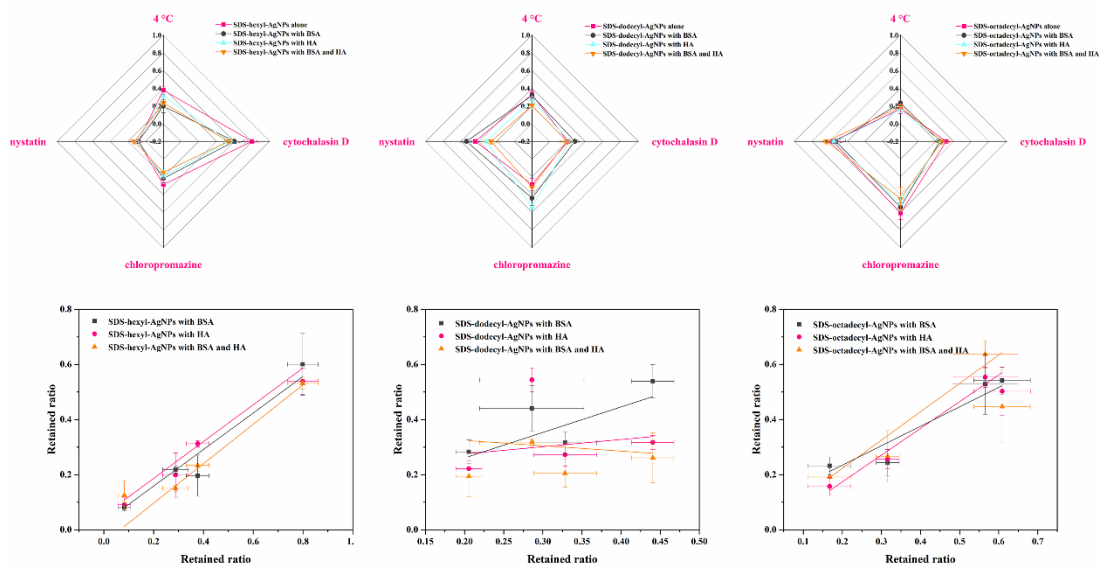


**Figure S7** The suppression effect of low temperature and pharmacological inhibitor (cytochalasin D, nystatin and chlorpromazine) on the bioaccumulation of SDS-alkyl-AgNPs alone or in the existence of organic matter (10 mg/L BSA, 10 mg/L HA or mixtures of 10 mg/L BSA and 10 mg/L HA) (upper graphs). Moreover, it was suggested that if NPs in the coexistence of organic matter followed the same uptake path as NPs alone, their retained ratio of Ag bioaccumulation under different inhibition condition should be correlated with NPs alone at the same condition. The linear correlation analysis was conducted for all the three NPs (down graphs). It was found that linear correlation ( $p < 0.05$ ) was established for SDS-hexyl-AgNPs and SDS-octadecyl-AgNPs, however not for SDS-dodecyl-AgNPs. It implied that organic matter would not affect the uptake path of SDS-alkyl-AgNPs and SDS-octadecyl-AgNPs but that of SDS-dodecyl-AgNPs.

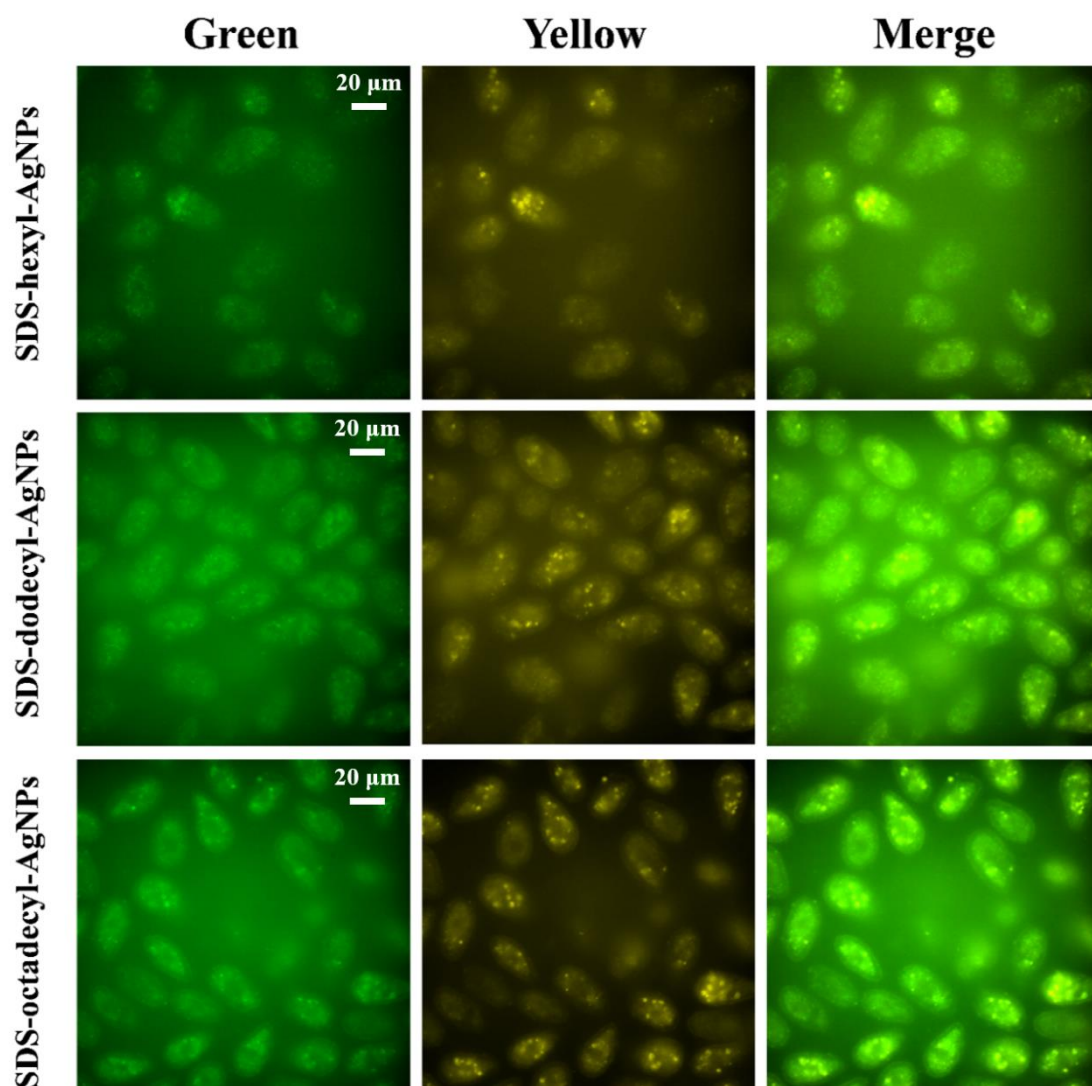


**Figure S8** The fluorescence images of *T. thermophila* under excitation wavelength of FITC and RBITC respectively. Cells were exposed with dual-fluorescence labelled NPs for 1 h before fixation. The images were merged to observed the overlap of fluorescent particles. The results strongly suggested the co-existence of fluorescent dyes on the nano-surface.

**Table S1** Residual ratio of SDS-alkyl AgNPs in 24-well plate after washing twice

	<i>SDS-hexyl-AgNPs</i>	<i>SDS-dodecyl-AgNPs</i>	<i>SDS-octadecyl-AgNPs</i>
<b>Residual ratio</b>	0.735%±0.096%	0.041%±0.015%	0.255%±0.147%

**Table S2** Dissolution ratio of SDS-alkyl AgNPs

	<i>SDS-hexyl-AgNPs</i>	<i>SDS-dodecyl-AgNPs</i>	<i>SDS-octadecyl-AgNPs</i>
<b>Dissolution ratio</b>	0.026%	0.228%	0.029%

**Table S3** Uptake rate of SDS-alkyl-AgNPs

<i>Sample</i>	<i>Uptake rate (ng/10<sup>5</sup> cell*h<sup>-1</sup>)</i>			
	<i>freshwater</i>	<i>freshwater with BSA</i>	<i>freshwater with HA</i>	<i>freshwater with BSA and HA</i>
SDS-hexyl-AgNPs	66.73±6.89	916.36±90.16	55.74±20.44	432.05±55.93
SDS-dodecyl-AgNPs	403.68±23.39	143.99±31.44	463.31±21.95	48.39±126.25*
SDS-octadecyl-AgNPs	407.38±82.24	125.91±14.31 <sup>^</sup>	ND	624.61±280.60*

\* represents Adjusted R-Square < 0.9. ND indicates that data could not be well fitted using a one-compartment kinetic model. <sup>^</sup> indicates that data was fitted using linear fitting.

## Reference

1. Y. Wan, Z. R. Guo, X. L. Jiang, K. Fang, X. Lu, Y. Zhang and N. Gu, Quasi-spherical silver nanoparticles: Aqueous synthesis and size control by the seed-mediated Lee-Meisel method, *J Colloid Interf Sci*, 2013, **394**, 263-268.
2. N. R. Jana and X. G. Peng, Single-phase and gram-scale routes toward nearly monodisperse Au and other noble metal nanocrystals, *J Am Chem Soc*, 2003, **125**, 14280-14281.
3. W. L. Li, L. D. Troyer, S. S. Lee, J. W. Wu, C. Kim, B. J. Lafferty, J. G. Catalano and J. D. Fortner, Engineering Nanoscale Iron Oxides for Uranyl Sorption and Separation: Optimization of Particle Core Size and Bilayer Surface Coatings, *Acs Appl Mater Inter*, 2017, **9**, 13163-13172.
4. W. L. Li, D. Liu, J. W. Wu, C. Kim and J. D. Fortner, Aqueous Aggregation and Surface Deposition Processes of Engineered Superparamagnetic Iron Oxide Nanoparticles for Environmental Applications, *Environmental Science & Technology*, 2014, **48**, 11892-11900.
5. W. L. Li, C. H. Hinton, S. S. Lee, J. W. Wu and J. D. Fortner, Surface engineering superparamagnetic nanoparticles for aqueous applications: design and characterization of tailored organic bilayers, *Environ Sci-Nano*, 2016, **3**, 85-93.
6. M. van de Weert and L. Stella, Fluorescence quenching and ligand binding: A critical discussion of a popular methodology, *Journal of Molecular Structure*, 2011, **998**, 144-150.